

A PARAMETRIC STUDY OF THE TUNNELING-INDUCED SURFACE SETTLEMENTS UNDER 3D CONDITIONS

Spiros A. Massinas¹, Michael G. Sakellariou¹

¹Department of Rural & Surveying Engineering
National Technical University of Athens
9 Iroon Polytechniou Street, Zografou Campus, Athens, Greece

Keywords: Tunneling, Shallow tunnels, Urban environment, NATM, Computational mechanics, 3D analyses, FDM

Abstract. *Complicated 3-Dimensional (3D) parametric analyses were carried out (by using Finite-Difference models of more than 80000 elements) in order to investigate the tunneling excavation and temporary support-induced surface settlements in the case of a shallow (depth 18m) tunnel (height 9m and width 18m), which is excavated by using the "NATM" method of tunneling. In the parametric studies the detailed excavation and temporary support of the tunnel is simulated, as well as diaphragm pile-walls that are used as temporary support for the excavation of deep pits. The position of the pile walls (in the parametric analyses) varies in both sides of the tunnel and is producing a geometrical asymmetry. As a result of the pile-walls presence in the sidewalls of the tunnel, a non-symmetrical shape of the surface settlement trough is obtained. The shape and the magnitude of the 3D settlement trough are calculated for different positions and stiffness of the pile-walls.*

1 INTRODUCTION

3-Dimensional (3D) analysis is used from many authors in order to investigate and to predict the tunneling excavation-induced surface settlements in the cases of shallow tunnels in urban environment. Several authors adopt a step-by-step approach, in which tunnel excavation is modeled by removal of tunnel face elements while installing temporary support measures (in case of NATM method) or installing a segmental lining (in case of TBM method), at a certain distance behind tunnel's face. Some other authors suggest the 3D modeling of a TBM excavation by applying a volume loss-control method as it is used in plane strain analysis, or by modeling the tunneling boring machine, such as shield, gap, grouting, face pressure etc. The scope of the most of the above-mentioned methods is the prediction of the 3D settlement trough for greenfield conditions or with the presence of buildings (Franzius and Potts, 2005).

The excavation and temporary support of a tunnel for greenfield conditions is a 3D problem, due to the presence of the excavation face in each excavation step. Nevertheless 2-Dimensional (2D) plain strain analysis instead of the step-by-step approach has been adopted by various authors to model tunnel excavation (due to the lack of computational time and resources), simulating the advance of the excavation face by relaxation of the stiffness of the elements of the face core or by applying a properly internal pressure P_i in the perimeter of the tunnel (M. Panet et al, 1987) or by controlling the ground volume loss, in each excavation step. It is evident that with the right assumptions and the right choice of the above parameters, in each excavation step, such an approach gives results (surface settlements) that are in good agreement with an equivalent 3D step-by-step analysis.

Nevertheless, in most cases the greenfield conditions are not the "real" conditions when tunneling in urban areas. Consequently the shape and the magnitude of the surface settlements in each side of the tunnel's axis are both non-symmetrical. The presence of buildings or other surface and subsurface structures are in most cases the geometrical parameters that lead to non-symmetrical shape and magnitude of the surface settlements. Such a case, with a large tunnel construction (by using the New Austrian Tunneling Method -NATM) next to existing subsurface structures, are examined and presented in the current study.

2 PROBLEM DESCRIPTION

There are cases, when tunneling in urban areas, that mined tunnels pass near deep diaphragm walls of existing subsurface structures (e.g. underground multi level parking), or very close to existing deep foundations of surface structures (e.g. pile foundations of buildings or bridges).

Moreover, in some other special cases, the construction of large underground station tunnels by using a Cut & Cover method is forbidden due to the presence of buildings (case A in fig. 1) or significant avenues (case B in fig. 1), in the surface along the axes of the tunnels. In such cases the whole station (including the main service building and the station tunnel with the ducts) is necessary to be constructed in parts, by applying the best construction method (e.g. the main service buildings with a Cut & Cover method by implementing anchored diaphragm pile-walls and the large station tunnel with conventional method such as NATM). In figure 1 the layout of such an underground station is presented.

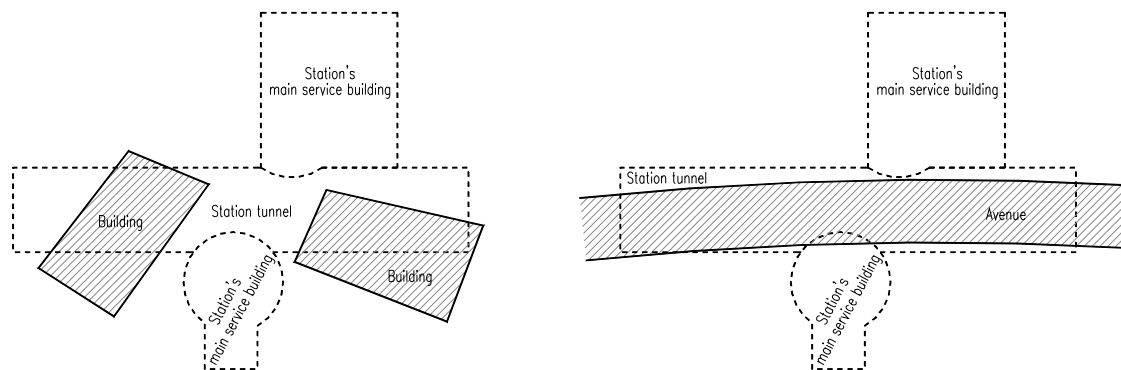


Figure 1. Layout of a typical underground station – Case A, buildings along tunnel's axis – Case B, significant avenue along tunnel's axis

A significant conclusion from the above mentioned cases is that the tunneling-induced surface settlement's shape and value will be non-symmetrical in each side of the tunnel's axis, due to stiffness contribution of the subsurface structures in tunnel's sidewalls.

This study presents results from a number of 3D Finite-Difference-Method (FDM) analyses (models sp1model2 to sp1model6 with more than 80000 elements) of a large station tunnel construction (by using NATM) next to existing diaphragm pile-walls (1m thick) with different configuration. The shape and as a result the stiffness of the pile-walls, as well as their position, varies in both sides of the tunnel producing in such way geometrical asymmetry. Finally, the results from an additional analysis (sp1model1) with a more complex station layout such as in case B of figure's 1 are presented. Important conclusions that came up from the analyses are presented in the relevant paragraphs below.

3 ANALYSIS DETAILS

3.1 Finite-Difference Program

All analyses were performed by using the Finite-Difference-Method (FDM) Program FLAC3D (Itasca Consulting Group, Inc.). The program uses the explicit, Lagrangian, calculation and the mixed-discretization zoning technique to model very accurately the plastic failure and flow. Explicit schemes can follow arbitrary nonlinearity in stress/strain laws in almost the same computer time as linear laws, whereas implicit solutions can take significantly longer time to solve nonlinear problems. It is not necessary to store any matrices and as a result of this, large models can be modeled with modest memory requirements. FLAC3D uses polyhedral (tetrahedral, hexahedral etc) elements which are called zones, for the generation of the 3D mesh-grid in order to model the soil or rock. Additional structural elements such as beams, cables, shells can be used in order to model structures that interact with the surrounding soil or rock.

3.2 Geometry

The geometry of the tunnel and the temporary support measures that are modeled in the 3D step-by-step analysis are presented in figure 2.

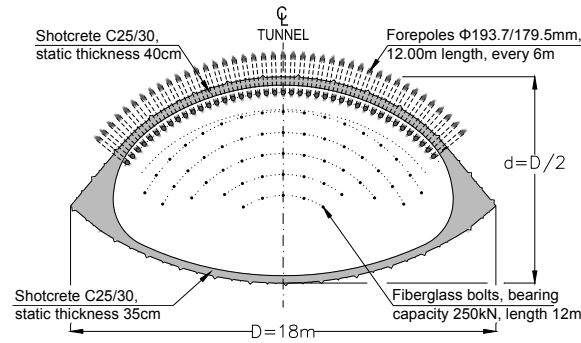


Figure 2. Geometry of tunnel and temporary support measures – Top Heading

In the analyses, only the excavation and temporary support of the Top Heading of the tunnel is simulated, due to the fact that this is the critical construction stage for a NATM tunnel constructed in two discrete phases (Top heading and Bench), concerning the induced surface settlements.

The overburden thickness of the tunnel in all analyses was $D=18\text{m}$ and the depth of the diaphragm pile-walls (d.p.-w.) $1.5 \times D=27\text{m}$ in analyses sp1model2 through sp1model6. In model sp1model1 the depth of the piles varied from D to $2 \times D$. The geometrical layout and parameters that are used in the analyses are presented in figure 3 and table 1.

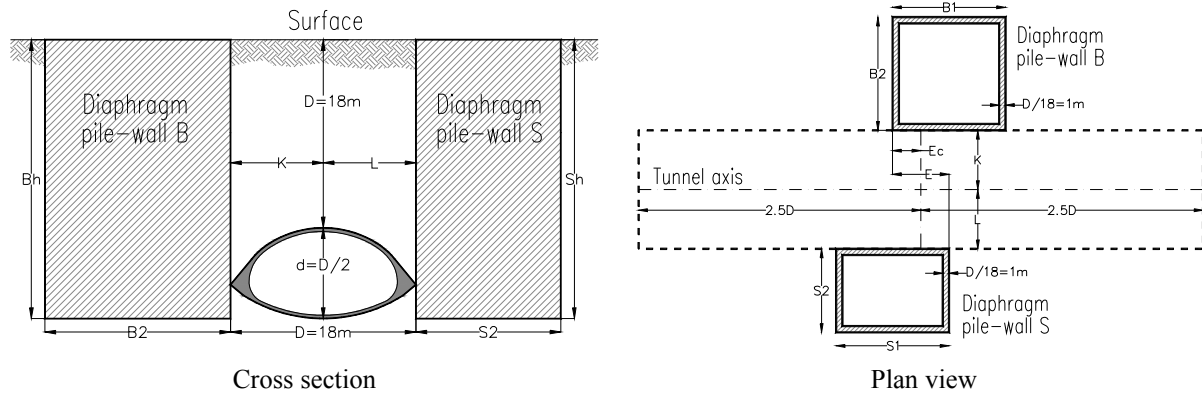


Figure 3. General geometrical layout for analysis

Analyses	Geometrical parameters (inputs)										Comments
	B1	B2	Bh	S1	S2	Sh	K	L	E	Ec	
sp1model2	-	-	-	-	-	-	-	-	-	-	Greenfield analysis
sp1model3	D	D	1.5D	-	-	-	0.5D	-	-	0.5D	Only d.p.-w. A is simulated
sp1model4	-	-	-	D	D	1.5D	-	0.5D	-	0.5D	Circular d.p.-w. B with outer diameter D. No d.p.-w. A is simulated.
sp1model5	D	D	1.5D	D	D	1.5D	0.5D	0.5D	0.5D	0.5D	Both d.p.-w. A & B are simulated.
sp1model6	D	D	1.5D	D	D	1.5D	0.5D	0.5D	0	0	Both d.p.-w. A & B are simulated.

Table 1 : Geometrical parameteres (inputs) for analysis

As regards analysis sp1model1, the underground complex station's layout-geometry is presented in a 3D FDM mesh (that is used for the analysis) in figure 4, due to the geometrical complicity of the layout. As it is clear from the figure, the left part of the tunnel and specifically part of the elephant foot type foundation of the temporary shotcrete shell, is connected with the diaphragm pile-walls (with rectangular shape in fig. 1) whereas the right part of the tunnel's temporary shotcrete shell is below a part of the right pile-wall (with circular shape and a rectangular part - see fig. 1).

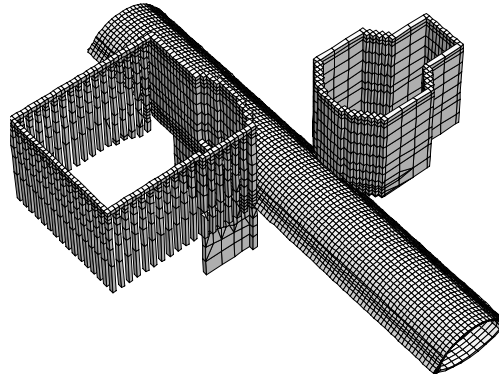


Figure 4. Complex 3D model of station (sp1modell analysis)

3.3 3D Model

The soil skeleton was modeled by using hexahedral zones, whereas the forepole grouted tubes were modeled by using beam structural elements and the fiberglass fully grouted bolts by using cable elements with interface, in order to simulate the interaction of the grout and the soil. For better simulation of the geometry of the temporary shotcrete shell hexahedral elastic zones were used with a Young's modulus of 10GPa and a Poisson's ratio 0.2. Intermediate values of Young's modulus were used for the simulation of the time dependent maturing of the green shotcrete. A rectangular coordinate system was used in this study with the y axis parallel to the tunnel axis and the positive z axis in the gravitational direction. The tunnel is constructed from the vertical start boundary $y=0\text{m}$ in the positive y-direction.

Because of geometrical asymmetry, the whole problem was modeled. In all vertical boundaries the horizontal movements normal to the boundary were restricted. On the bottom boundary, soil movements were restricted in all directions. In order to avoid any effects in the surface settlements shape and magnitude, due to boundaries position, the proper grid dimensions were implemented in the models. Thus, for the vertical boundaries normal to x-direction, a distance of $10xD$ from each side of the centerline of the tunnel was selected and also a distance of $2xD$ for the extension of the grid below tunnel springline, as proposed by Oteo & Sagaseta (1982), observed by Burd et al. (1994), studied by C.H. Pang, K.Y. Yong (Some considerations in finite element analysis of tunneling 2005, National University of Singapore) and ensured by the authors of this paper with parametric analyses that are not presented in this study. As it regards the distance between the vertical boundary normal to y-direction in front of tunnel's face and the final excavation face, $10xD$ proved to be a sufficient value.

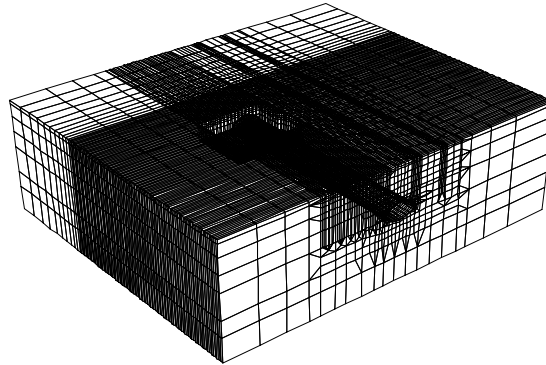


Figure 5. Typical part of a 3D finite-difference grid

3.4 Tunnel Excavation

The 3D tunnel excavation was modeled by using a step-by-step approach. In each increment of the analysis, soil excavation was simulated in front of the tunnel face and certain layers of the shotcrete shell were implemented in proper distances behind the tunnel face according to the simulated construction sequence. The excavation step (Exc.S.) was 1m. Every six (6) Exc.S. the installation of a new forepole umbrella was simulated in front of tunnel's face. The application of the fiberglass bolts was simulated also every six (6) Exc.S. but in different time with the umbrella installation. The closure of the temporary invert, 3m behind the excavation face, was simulated every six (6) Exc.S. along with the forepoles application.

The same sequence of tunnel excavation was implemented in all six (6) analyses.

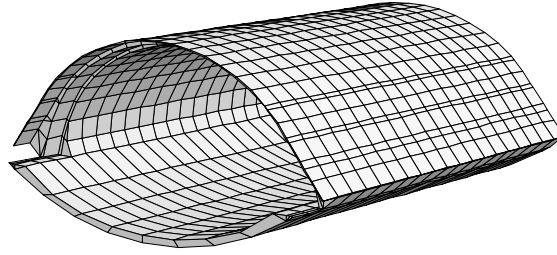


Figure 6. Typical view of the simulated 3D tunnel's shotcrete shell

3.5 Soil Model

The soil profile consisted of conglomerates and marls with small intercalations of sand and clay, was represented by an elastoplastic model. A Mohr-Coulomb surface modeled the plastic behavior of the soil skeleton (non-associated flow rule for shear failure and associated rule for tension failure). The geotechnical parameters are presented in table 2. The coefficient of lateral earth pressure at rest was $K_0=0.5$.

Depth	Geotechnical Parameters			
	Young's Modulus E (MPa)	Friction angle ϕ (°)	Cohesion c (kPa)	Unit weight γ (kN/m ³)
0 - 2m	20	32	5	20
2 - 16.5m	30	24	10	20
>16.5m	380	28	23	23

Table 2 : Geotechnical parameters of soil profile

4 PARAMETRIC STUDY

4.1 Greenfield Analysis

A number of greenfield (no d.p.-w.) grids were analyzed in order to ensure the proper grid dimensions for the parametric study (described in paragraph 3.3). The analyzed grids showed that steady-state conditions in surface settlements were reached approximately $3xD$ behind the tunnel face after the excavation of the tunnel over a length of 90m. Thus, according to final greenfield analysis (see fig. 7, sp1model2) a total tunnel excavation length of 90m simulated in analyses sp1model3 to sp1model6.

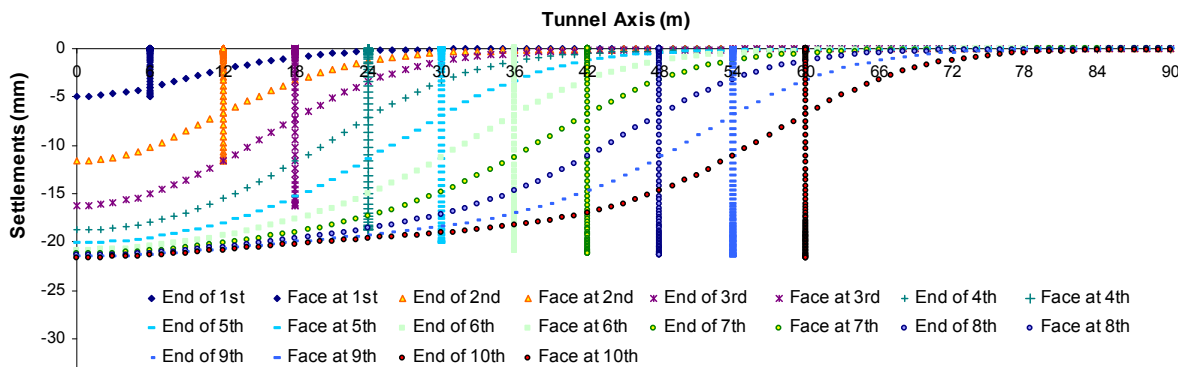


Figure 7. Development of longitudinal surface settlement profile with tunnel progress for greenfield analysis sp1model2

In the diagram of figure 7 the expressions e.g. “End of 3rd” and “Face at 3rd” (vertical lines) means “end of the excavation of the 3rd umbrella”, thus 18m of tunnel's excavated length and “the face of the tunnel is at the end of the 3rd umbrella”, thus at position $y=18m$, respectively.

According to greenfield analysis results, the maximum calculated surface settlements are approximately 21mm. It is evident that the distribution of the maximum surface settlements lies along a line which is equal to tunnel axis and will be referred to as the critical trail (see figure 8). As it will be described later on, the critical trail is diverted from the tunnel axis or rotated through a point of inflection, when the tunnel excavation is realized near existing subsurface structures (in this study near d.p.-w).

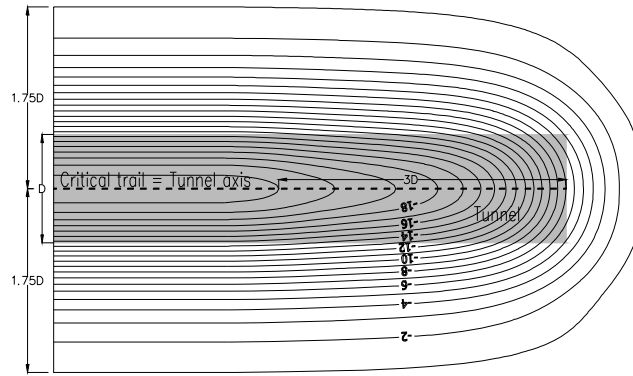


Figure 8. Tunnel-induced surface settlements – Critical trail – Sp1model2

4.2 Analyses Results – Sp1model3 and Sp1model4

The presence, in the one side of the tunnel's sidewalls, of a rectangular/circular shape diaphragm pile-wall in analyses sp1model3 and sp1model4 respectively, produces geometrical disturbance in the distribution of the surface settlements, as presented in figure 9, as well as reduction to the magnitude of the expected settlements. Specifically the critical trail was diverted from the tunnel's centerline for a total length $div > B1$ (for $B1$ see fig. 3 and table 1) due to the stiffness and the shape of the d.p.-w. The diversion was realized to the opposite side of the d.p.-w. The point of maximum diversion, as it is presented in figure 9, laid in the intersection point of the critical trail and the iso-stiff line, which is the theoretical line that separates imaginably the stiffness of the d.p.-w. in equal parts.

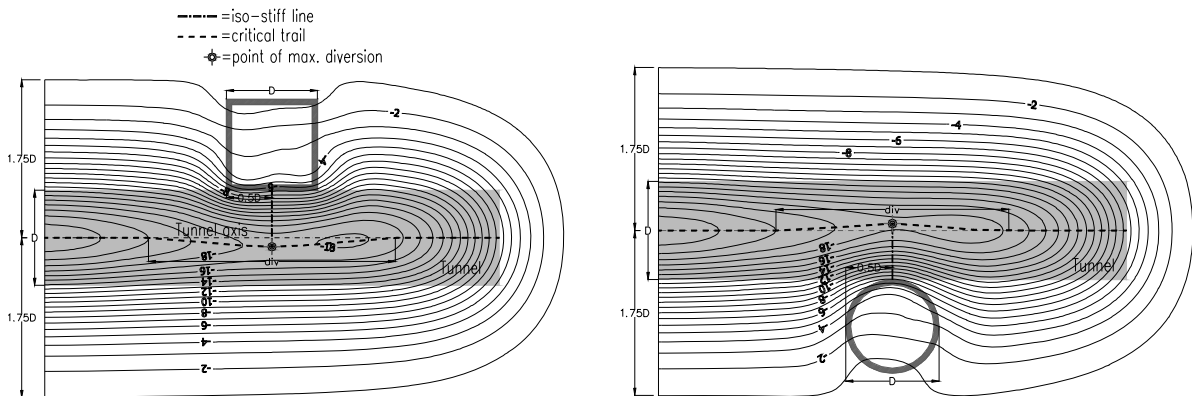


Figure 9. Tunnel-induced surface settlements– Critical trail and iso-stiff line – Sp1model3 and Sp1model4

As regards critical trail, it is stated that can be described with accuracy by the mathematical description of a Gaussian error function. Following this approach, the horizontal diversion of the critical trail from the tunnel's axis is given by

$$\omega_d(y) = \omega_{d,max} \cdot e^{\frac{-y^2}{2\sigma^2}} \quad (1)$$

where $\omega_{d,max}$ is the maximum diversion from tunnel axis, along iso-stiff line. The parameter σ , which represents the points of inflection of the curve, is the distance (along tunnel axis) of the iso-stiff line from the ends of the diaphragm pile-walls (thus in this case $\sigma=0.5xD$) approximately.

The maximum diversion $\omega_{d,max}$ is depended on the shape and the stiffness of the subsurface structure (e.g. diaphragm pile-wall), it's distance from the tunnel axis, the shape and the dimensions of the tunnel, as well as the soil profile. It is evident that the greater the $\omega_{d,max}$ is, the smaller the surface settlements are, along critical trail (in the area with the maximum diversion). For example, in analyses sp1model3 and sp1model4, $\omega_{d3,max}=1.8m$ and $\omega_{d4,max}=1.3m$ respectively, whereas the maximum surface settlements are 17mm and 18mm respectively. It is noted that due to the presence of the d.p.-w. a reduction to the magnitude of the settlements (in the area of $\omega_{d,max}$) was calculated approximately 15% and 10%, for cases sp1model3 and sp1model4 respectively. Development of the longitudinal surface settlements along tunnel axis, with more intense reduction to the settlements magnitude, is presented in paragraph 4.3 for case sp1modell1.

4.3 Analyses Results – Sp1model5, Sp1model6 and Sp1model1

In analyses sp1model5 and sp1model6 the induced surface settlements and the shape of the critical trail were examined due to the presence of diaphragm pile-walls in both sides of the tunnel. The geometrical disturbance in the distribution of the surface settlements as well as the reduction of the settlements magnitude was more intense than in previous-presented analyses.

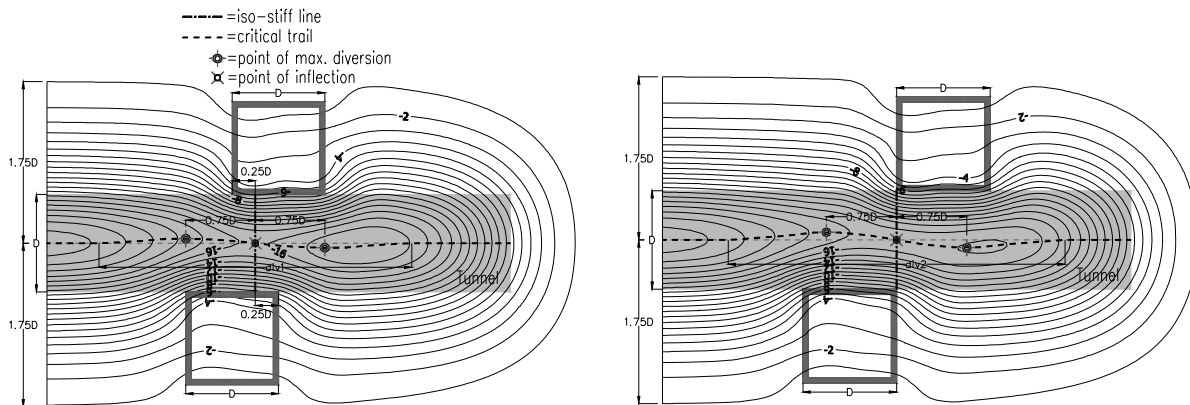


Figure 10. Tunnel-induced surface settlements – Critical trail and iso-stiff line – Sp1model5 and Sp1model6

The inflection point presented in figure 10 is a new crucial mark because the critical trail rotates through it, thus producing a symmetrical diversion of the maximum settlement path in each side of the iso-stiff line. It is evident that the above-mentioned symmetry is due to the same shape of the opposite diaphragm pile-walls as well as their equal perpendicular distance from the tunnel axis. As it is evident from the analyses, the more the distance E (see table 1) increases, the more the surface settlements, $\omega_{d,max}$ and distance div (see fig. 10) reduces. It is noted that parameter div is the length of the disturbed critical trail. For example in sp1model5 and sp1model6, $div1$ is approximately $3.3xD$ and $div2$ $3.7xD$ respectively.

It is important to point out that in different cases (such as in analysis sp1model1) with complicate shapes of subsurface structures and generally speaking without the symmetrical geometric requirements of analyses sp1model5 and sp1model6, the position of the inflection point may not lie along tunnel's axis, but is more probable to have an eccentricity. In such cases the iso-stiff line cannot be defined properly. Moreover, the rotation of the critical trail through the inflection point cannot be symmetrical, producing in such way different $\omega_{d,max}$ that are depending on the stiffness contribution, along tunnel's axis, of the subsurface structures in each side of inflection point. Indeed, it is certainly that the new inflection point will be inside the area where there is stiffness concentration from both subsurface structures. For stressing the above statement, the tunnel-induced surface-settlements, of analysis sp1model1, are presented in figure 11 along with the inflection point.

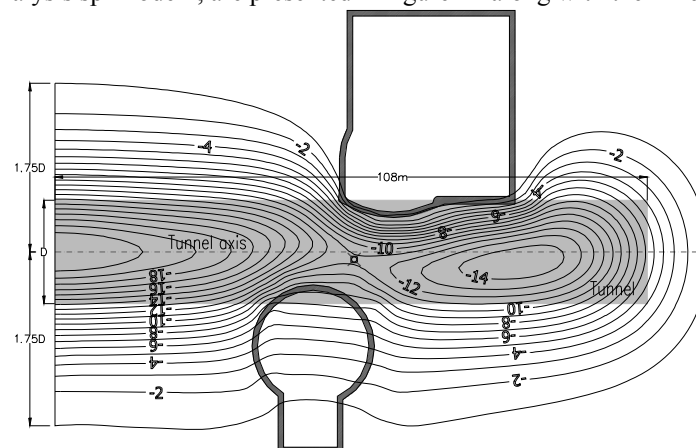


Figure 11. Tunnel-induced surface settlements – Point of inflection – Sp1model1

As it is evident from the settlement contours, the diversion of the critical line is greater in front of the rectangular shape d.p.-w. than in the area in front of the circular shape d.p.-w. The greater the stiffness contribution, along tunnel's axis, of the subsurface structures is, the greater the diversion is.

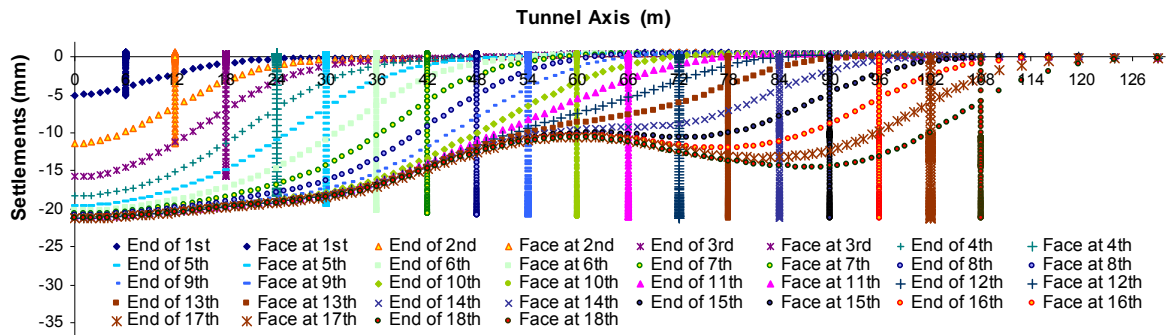


Figure 12. Development of longitudinal surface settlement profile with tunnel progress for analysis sp1modell

In the diagram of figure 12 it is shown the reduction of the magnitude of the surface settlements along tunnel's axis in comparison with the greenfield analysis (see fig. 7), of approximately 35%. The calculation time for analysis sp1modell, consisted of 126614 zones and 9025 structural elements, was 151h (performed on an Intel Celeron 2.5GHz, 2x256 DDR SDRAM).

5 CONCLUSIONS

This paper presents 3D surface settlements results from a number of 3D FDM studies of a tunnel excavation near subsurface structures (d.p.-w.). The detailed step-by-step excavation and temporary support of the NATM tunnel (with Exc.S 1m) is simulated as well as the d.p.-w. The position of the d.p.-w. varies in both sides of the tunnel producing geometrical disturbance in the distribution of the surface settlements, which is described by three parameters, the critical trail the iso-stiff line and the diversion ω_d . The second parameter is showed that is well-described by the mathematical description of a Gaussian error function, for cases with subsurface structures in one side of the tunnel.

Moreover, in cases with subsurface structures in both sides of the tunnel with same shape and equal perpendicular distance from the tunnel axis a new parameter is introduced. The inflection point is a new crucial mark because the critical trail is rotated through it, producing in such way symmetrical diversion of the maximum settlement path in each side of the iso-stiff line.

For more complex subsurface structures, without symmetrical geometric requirements, it is showed that the rotation of the critical trail through the inflection point is not symmetrical, producing in such way different $\omega_{d,max}$ that depends on the stiffness contribution, along tunnel axis, of the subsurface structures in each side of inflection point. In addition, it is stated that the new inflection point lies inside the area where there is stiffness concentration from both subsurface structures.

In conclusion it is noted that the detection of the critical trail with the above-presented methodology is important, because it gives in principle, a quick estimation of the shape of the 3D tunneling-induced surface settlement through due to the presence of the subsurface structures, prior to the implementation of a detailed 3D analysis. The definition of $\omega_{d,max}$ is under research and will be presented in a sequential publication.

6 REFERENCES

- [1] Gonzalez, C. & Sagaseta, C. Patterns of soil deformation around tunnels. Application to the extension of Madrid Metro. *Computers and Geotechnics* 28 (2001) 445-468.
- [2] Franzius, J.N & Potts, D.M. Influence of Mesh Geometry on Three-Dimensional Finite-Element Analysis of Tunnel Excavation. *International Journal of Geomechanics*, ASCE, September 2005.
- [3] Massinas, S., Koronakis, N. & Kontothanassis, P. Design and construction of an underground station tunnel with interconnected galleries for achieving high advance rates and controlling settlements. *Underground Construction*, London, October 2005.
- [4] Oteo, C.S. & Sagaseta, C. Prediction of settlements due to underground openings. *International Symposium on Numerical Models in Geomechanics*, Zurich, 13-17 September 1982, 653-659.
- [5] Panet, M., Sulem, J. & Guenot, A. An analytical solution for time-dependent displacements in a circular tunnel. *Int. J. Rock Mech. Min. Sci. & Geomech. Abstr.* Vol. 24, No. 3, pp. 155-164, 1987.
- [6] Pang, C.H., Yong, K.Y. & Dasari, G.R. 2005. Some considerations in finite element analysis of tunneling. *Underground Space Use: Analysis of the Past and Lessons for the Future*, ITA-AITES, Turkey, 2005.